



## Technical Note: Semi-rigid chambers for methane gas flux measurements on tree stems

Andy Siegenthaler, Bertie Welch, Sunitha R. Pangala, Michael Peacock, and Vincent Gauci

Centre for Earth, Planetary, Space & Astronomical Research, Department of Environment, Earth & Ecosystems, The Open University, Milton Keynes, UK

Correspondence to: Andy Siegenthaler (mbee777@gmail.com)

Received: 22 August 2015 – Published in Biogeosciences Discuss.: 29 September 2015

Revised: 17 January 2016 – Accepted: 14 February 2016 – Published: 26 February 2016

**Abstract.** There is increasing interest in the measurement of methane ( $\text{CH}_4$ ) emissions from tree stems in a wide range of ecosystems so as to determine how they contribute to the total ecosystem flux. To date, tree  $\text{CH}_4$  fluxes are commonly measured using rigid closed chambers (static or dynamic), which often pose challenges as these are bulky and limit measurement of  $\text{CH}_4$  fluxes to only a very narrow range of tree stem sizes and shapes. To overcome these challenges we aimed to design and test new semi-rigid stem-flux chambers (or sleeves). We compared the  $\text{CH}_4$  permeability of the new semi-rigid chambers with that of the traditional rigid chamber approach, in the laboratory and in the field, with continuous flow or syringe injections. We found that the semi-rigid chambers had reduced gas permeability and optimal stem gas exchange surface to total chamber volume ratio ( $S_c / V_{\text{tot}}$ ) allowing better headspace mixing, especially when connected in a dynamic mode to a continuous flow gas analyser. Semi-rigid sleeves can easily be constructed and transported in multiple sizes, are extremely light, cheap to build and fast to deploy. This makes them ideal for use in remote ecosystems where access logistics is complicated.

bers adapted to various tree-stem sizes. Presently, the most common chambers used to measure  $\text{CH}_4$  emissions from tree stems are closed rigid chambers in the form of either a vertical cylinder, a horizontal cylinder or a cube fitted around tree stems (e.g. Gauci et al., 2010; Pangala et al., 2013; Terazawa et al., 2007; Hari et al., 1991; Rusch and Rennenberg, 1998). These chambers can be deployed either vertically by enclosing the whole stem or, alternatively when the stems are too large, laterally on the stem, covering only a small fraction of the stem surface (e.g. Levy et al., 1999; Teskey and McGuire, 2005; Ryan, 1990; Hari et al., 1991). These techniques were originally designed to measure  $\text{CH}_4$  and carbon dioxide ( $\text{CO}_2$ ) from samples manually taken with syringes and analysed by gas chromatography. The ratio between the gas exchange surface and the chamber volume ( $S_c / V_{\text{tot}}$ ) was transposed from soil chambers and was not necessarily adapted to the lower fluxes found in tree stems, and are therefore often too high (Hutchinson and Livingston, 2001). In other words, if the chambers are too large for a given exchange surface, mixing problems may occur, making it important to circulate the air in their headspace (Hutchinson and Livingston, 1993; Rusch and Rennenberg, 1998).

With the advent of continuous flow analytical techniques and increasing precision of instruments (e.g. cavity ring-down spectroscopy, infrared and photo-acoustic gas analysers), the need for longer accumulation periods to detect significant concentration changes has become obsolete. The tendency is to reduce the accumulation period as much as possible in order to be able to use more straightforward linear regressions to determine fluxes closest to the point of chamber closure. Unlike open chamber techniques which allow steady-state measurements (e.g. Bortoluzzi et al., 2006; Nor-

### 1 Introduction

Recent research into ecosystem greenhouse gas fluxes has shown that tree stems emit significant amounts of methane ( $\text{CH}_4$ ; Terazawa et al., 2007, 2015; Rusch and Rennenberg, 1998; Gauci et al., 2010; Pangala et al., 2013; Rice et al., 2010) although the transport mechanisms and global importance of tree-mediated emissions remain largely unknown. These past investigations have used a variety of closed cham-

man et al., 1997; Subke et al., 2003; Pumpanen et al., 2004), closed chambers are non-steady state systems; the diffusive laws advocate the use of non-linear regressions of gas concentrations as a function of time to determine rates, as these decrease with increasing gas saturation (Hutchinson and Livingston, 2001; Pihlatie et al., 2013; Pumpanen et al., 2004; Kutzbach et al., 2007).

With continuous flow gas analysers there are three main advantages: (1) they are non-dispersive as no gas needs to be taken out of the measurement system and irreversibly “consumed”, (2) they circulate air between the chamber and the gas detectors, which for small chamber volumes could represent enough mixing to avoid underestimations of fluxes by as much as 36 to 58 % in non-mixed soil-atmosphere exchanges (Christiansen et al., 2011), and (3) with measurement frequencies of up to 10 Hertz and precisions of  $\pm 2$  ppb the closure time needed to get a representative accumulation slope has been dramatically reduced using these devices (excluding the equilibration period) and therefore it also avoids underestimations due to regressions made over longer periods of time (Hutchinson and Livingston, 2001; Pihlatie et al., 2013). In addition, recent work has focused on trace gases (e.g. CH<sub>4</sub> and N<sub>2</sub>O) which have lower accumulation rates compared to the more frequently measured CO<sub>2</sub> (IPCC, 2007), moderating the saturation issue inherent to non-steady state setups (Hutchinson and Livingston, 2001). Altogether, these point towards the use of a smaller stem chamber with larger gas exchange surface per chamber volume proportion ( $S_c / V_{\text{tot}}$  ratio).

A further complicating factor is field access. Stem-methane emissions have recently begun to be investigated in remote areas such as in forested tropical wetlands with often no road access. In those areas it is a logistical challenge to carry large and/or heavy loads. Moreover, because of the great variety of stem sizes and/or shapes, a whole collection of rigid chambers is usually needed to cover most of the ecosystem tree species thus creating further logistical and cost issues.

In order to meet the new challenges presented by the growing interest in measuring greenhouse gas fluxes from tree stems we aimed to design, describe and test/deploy new semi-rigid stem-emission chambers in the laboratory and in the field, and to compare their permeability to CH<sub>4</sub> (gas conductance) with previously described rigid chambers. Thus far, semi-rigid sleeve chambers have been used effectively in several of our measurement campaigns. We therefore consider their detailed reporting to be of interest to a broader constituency of eco-physiologists and biogeochemists. We also examine various methodological benefits and logistical advantages of using this new approach.

## 2 Materials and methods

### 2.1 Chamber designs: semi-rigid sleeve and rigid chamber

Our approach to measure stem CH<sub>4</sub> emissions, which could also include other greenhouse gases produced in anaerobic conditions such as N<sub>2</sub>O, uses a semi-rigid chamber (or sleeve). The preferred material was a pre-shaped and gas impermeable PET (polyethylene terephthalate) or PC (polycarbonate) plastic sheet with a natural tendency to curve induced by 3–4 vertically distributed imprinted rims on the periphery. These rims ensured good stability and helped maintain the desired natural curvature of the sleeve that proved to be very helpful for the deployment of the sleeves on the stems as the sleeve could hold in place without straps.

To investigate permeability changes due to both the size and the approach, we used two semi-rigid sleeves together with a rigid chamber. As this was straightforward, for the smaller semi-rigid sleeve we sourced the pre-shaped material from a cylindrical 3 L soft drink bottle, which already had the desired imprinted rims. The 0.1 mm thick bottle was truncated above and below the cylindrical section, and opened vertically on the side. For the larger sleeve we sourced the material from 0.2 mm thick not pre-shaped semi-rigid PC sheets. Both types of plastic sheets have very low gas permeabilities under experimental standard ambient temperature and pressure (SATP from UIPAC) conditions and short chamber enclosure times (McKeen, 2012).

The edges of the sheets were framed with 1.5 cm thick and 3 cm wide adhesive backed expanded Neoprene strips (Seals+Direct Ltd, Hampshire, UK); closed cell neoprene foam that is gas tight and can be bent, but is hardly compressible ( $\leq 3$  % with 200 N). This Neoprene strip was placed as a frame around the rectangular sheet to provide a seal and to ensure a constant volume between the sheet and the tree stem (Fig. 1). The adhesive was provided on one side of the expanded Neoprene strips. Inside this framed volume we placed two Neoprene vertical wedges (1.5 cm thick and 3 cm wide) to keep the sheet equidistant from the stem all along the radial periphery of the sleeve. The sleeve was also equipped with two snap-on rubber caps with inserted three-way Luer-lock stopcocks (BBraun, Bethlehem, USA) that permitted connection to the Ultraportable Greenhouse Gas Analyser (UGGA, Los Gatos Research Inc., Mountain View, USA) via two 4.6 m long and 5 mm inside diameter PTFE (polytetrafluoroethylene) coated PVC (polyvinyl chloride) parallel tubes (Nalgene, Rochester, USA). As venting was recommended (Hutchinson and Livingston, 2001; Christiansen et al., 2011), both sleeves were equipped with a coiled vent tube (18 cm long, 1.2 mm inner diameter). We downscaled the vent described by Hutchinson and Livingston (2001) by a factor 48 in terms of vent volume whereas the sleeves were a factor 10 to 20 less voluminous as compared to the authors' chamber (14 L). Their study showed that in a

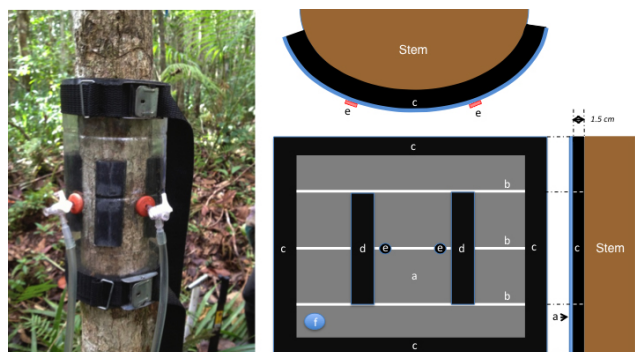


**Figure 1.** Smaller semi-rigid stem sleeve attached to a stem. The plastic PET sheet (a) has three imprinted circular rims (b) that ensured good stability and natural curvature of the sleeve. The circumference of the sheet was framed with a 1.5 cm thick and 3 cm wide expanded Neoprene strip (c) that sealed off the headspace located between the sheet and the stem. Inside this volume there were two vertical wedges (d) that kept the sheet at equidistance from the stem along the radial periphery of the sleeve. In its centre the sleeve was equipped with two snap-on rubbers with inserted three-way stopcocks (e) that were further connected to PVC tubes that went from the sleeve to the Ultraportable Greenhouse Gas Analyser. A coiled vent was placed in one corner of the sleeve (f) to regulate the pressure. The chamber was tightened to the stem with the help of two straps that perfectly aligned on top of the horizontal strips.

perfectly sealed chamber, after 30 min of deployment the gas mass loss through the sole vent represented 0.038 % of the target gas.

We tested all the components of the semi-rigid sleeves independently for unwanted background contaminations that could interfere with CH<sub>4</sub> emissions from the stems by incubating them for 2 hours in 500 mL borosilicate glass beakers filled with air and connected in continuous flow with the UGGA. The selected raw material was inert and did not interfere with measurements from the environment. We also tested the compressibility of sleeves by pulling the straps with a 200 N force (twice 100 N) and measuring the thickness of the Neoprene frame before and after pulling (Fig. 2, see also chamber deployment section).

We also compared the CH<sub>4</sub> losses from our new semi-rigid sleeves with a previously used rigid chamber design, similar to the ones constructed and described in other studies (Rusch and Rennenberg, 1998; Gauci et al., 2010; Pangala et al., 2013). The closed rigid chamber was constructed from cylindrical Perspex® (Perspex, Tamworth, UK) of inner diameter of 28 cm and had an inner height of 30 cm. The cylinder was cut into two halves, which were held together with a metal hinge. The two half-cylinders were framed within a 5 cm wide and 1 cm thick frame made of flat Perspex® that was fitted with Neoprene strips. The cylindrical chamber had a central opening to enclose the tree stem. Two smaller cylinders (18 cm diameter × 5 cm height) were attached on either side of that opening (Fig. 3). The chamber was equipped with

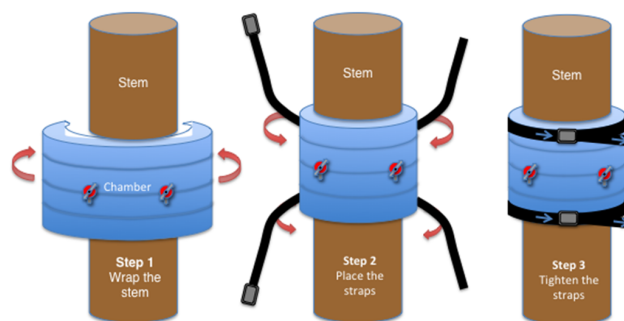


**Figure 2.** The three steps of the semi-rigid stem sleeve deployment. To ensure a good contact between the frame strips and the stem it was important to distribute the pressure of each strap all around the frames' periphery when tightening the sleeve. Close to the centre two snap-on rubbers with inserted three-way stopcocks were pressed into the PET or PC plastic sheet. These stopcocks were connected to the two PVC tubes that circulated air in a continuous flow mode when connected to an Ultraportable Greenhouse Gas Analyser (UGGA).

a gas sampling port and a small vent tube (12 cm long; 6 mm diameter).

## 2.2 Enclosed chamber volume and gas exchange surface determinations

The volume of the semi-rigid sleeves could be determined precisely in two different ways. Firstly, we extrapolated the empirical total chamber volume ( $V'_{\text{tot}}$ ) from the CH<sub>4</sub> concentration dilution factor after having inserted a known volume ( $V_{\text{standard}}$ ) of a 2000 ppmv CH<sub>4</sub> standard (Air Liquide, Paris, France) into the sleeve's enclosed volume and measuring the end concentration ( $C_0$ ) after dilution, and subtracting the atmospheric CH<sub>4</sub> concentration ( $C_{\text{atm}}$ ) originally in the chamber. The two semi-rigid sleeves and a rigid chamber were attached to an inert stainless steel cylinder (see chamber deployment). The dilution was done in 90 s so that the losses through gas permeability of the chambers remained negligible. This extrapolation was formalised as

$$V'_{\text{tot}} = V_{\text{standard}} \times \frac{(C_{\text{standard}})}{(C_0 - C_{\text{atm}})}. \quad (1)$$

Secondly, we also calculated the theoretical volume of the sleeves ( $V_c$ ) by subtracting a sector ( $K$ ) of both, a smaller cylinder volume ( $V_{\text{stem}}$ ) from a larger cylinder volume ( $V_{\text{ext}}$ ), minus the volume taken by the vertical wedges ( $V_{\text{wedges}}$ ; Fig. 4). The sector ( $K$ ) was determined from a ratio between the sleeve length ( $L$ ) and the circumference at the external edge of the sleeve ( $\pi D_{\text{ext}}$ ). The sleeve length ( $L$ ) is the length of the incompressible external edge of the chamber and represents a fraction of the total circumference given by  $\pi D_{\text{ext}}$ . The diameter of the smaller cylinder (the compressible internal foamy edge) is given by the diameter of the stem ( $D_{\text{stem}}$ ). The larger cylinder diameter ( $D_{\text{ext}}$ ) is the diameter given by

the stem ( $D_{\text{stem}}$ ) plus the thickness ( $T$ ) of the sleeve. Both cylinders have the same height ( $H$ ). Thereafter, we have

$$D_{\text{ext}} = D_{\text{stem}} + 2T \quad (2)$$

$$K = \frac{L}{\pi D_{\text{ext}}} = \frac{L}{\pi (D_{\text{stem}} + 2T)} \quad (3)$$

$$V_c = K (V_{\text{ext}} - V_{\text{stem}}) - V_{\text{wedges}} = \frac{HL}{(D_{\text{stem}} + 2T)} \times \left[ \left( \frac{D_{\text{stem}} + 2T}{2} \right)^2 - \left( \frac{D_{\text{stem}}}{2} \right)^2 \right] - V_{\text{wedges}}. \quad (4)$$

However, the total volume ( $V_{\text{tot}}$ ) is the sum of the chamber volume ( $V_c$ ) plus the dead volume enclosed in the gas analyser and the tubes ( $V_{\text{dead}}$ ):

$$V_{\text{tot}} = V_c + V_{\text{dead}}. \quad (5)$$

Similarly, the gas exchange surface of the sleeves ( $S_c$ ) was calculated by considering the sector ( $K$ ) of the stem surface ( $S_{\text{stem}}$ ) covered by the chamber at the circumference of the stem ( $\pi D_{\text{stem}}$ ) and the height of the sleeve ( $H$ ), minus the small surface covered by the vertical wedges ( $S_{\text{wedges}}$ ):

$$S_c = K \times S_{\text{stem}} - S_{\text{wedges}} = \frac{HL}{(D_{\text{stem}} + 2T)} \times D_{\text{stem}} - S_{\text{wedges}}. \quad (6)$$

### 2.3 Chamber deployment

The three types of chambers (two semi-rigid sleeves and one rigid chamber) were deployed on a gas-inert stainless steel cylinder of diameter 15 cm. The semi-rigid chambers were flattened around the cylinder and subsequently attached and tightened with two metal cam straps at the top and bottom of the frame (Fig. 2). The straps were 1.5 m long and 3 cm wide. An additional strap was necessary at mid-height of the bigger sleeve to ensure a good cohesion of the vertical Neoprene frames and vertical wedges with the stem (steel cylinder in this case).

Before installing the rigid acrylic chamber, closed cell Neoprene foam bands (7 cm wide and 4 cm thick) were attached at the bottom of the inert stainless steel cylinder and also at 35 cm height using double-sided Scotch tape (3M, St-Paul, USA) to append the extremities of the band as well as packing brown tape (5 cm wide) to tighten the band firmly against the metallic cylinder. The two mobile panels of the chamber were opened and the upper and lower half-necks of one panel were lodged around the two foam bands by compressing the foam so as to ensure gas tightness. Finally, all open-end flanges surrounding the cylindrical volume were progressively closed with Handy-grips (Irwin, Vernier, Switzerland).

We used the larger semi-rigid chamber to exemplify the field deployment (Table 1). We deployed it on 12 tree stems

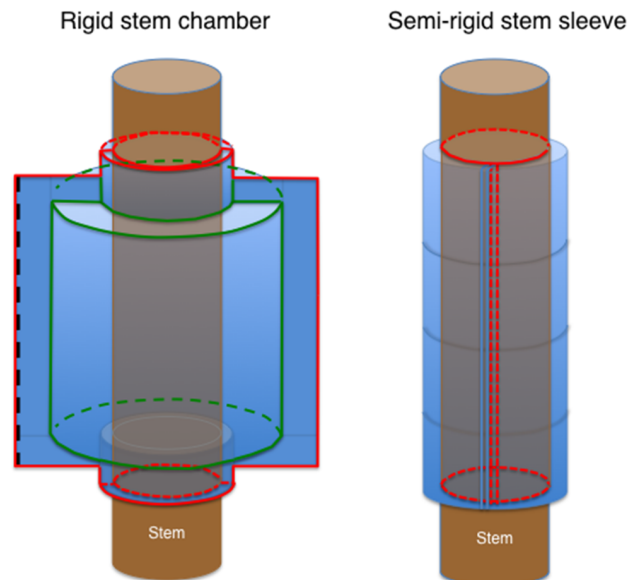


**Figure 3.** Potential air contact path lines (chamber air versus ambient air) where gas diffusion can occur; a comparison between the acrylic rigid cylinder approach and the semi-rigid sleeve approach. The red lines represented the mobile contact lines that needed to be sealed properly every time the chambers were deployed and where most of the losses were likely to occur. The green lines represented the fixed contact lines which could have been leaking as a result of twisting forces on the joints leading to cracks.

(diameter at breast height: 25–45 cm) located in the northern boreal zone (*Pinus sylvestris* and *Betula pendula*, Degerö mire, Sweden) as well as in a tropical lowland forest (*Heisteria concinna*, Barro Colorado Island, Panama). The sleeves were placed at mid-height on the stems at 35 cm of height. We shaded the sleeves with a plasticised aluminum foil to minimise any changes to chamber temperature which might otherwise affect stem-gas exchange processes. In the lab this measure was unnecessary. We tested the sleeve's CH<sub>4</sub> concentration change on both, very smooth birch stems and very rough pine-tree stems to contrast the concentration readings as much as possible. To ensure optimal gas tightness it was important to distribute the pressure of each strap all around the surface of the sleeve. We visually checked for gaps between the stem and the Neoprene strips. Monitoring the CH<sub>4</sub> concentration change in a continuous flow mode made an optimal gas tightness test. A leaking chamber (mainly pressure-driven bulk flow following Hagen-Poiseuille's law) typically displayed fluctuating concentrations with concentration build-up being recurrently drawn down. Finally, we also used the larger semi-rigid sleeve together with a manual syringe sampling. For that purpose we used a 30 mL plastic syringe fitted with a Luer-lock three-way stopcock (BBraun, Bethlehem, USA) and connected it to one of the two stopcocks on the sleeve. At  $t = 0$ ,  $t = 5$ ,  $t = 10$  and  $t = 15$  min we collected 12 mL of gas sample from the sleeve and trans-

**Table 1.** Chamber dimensions and mean permeabilities ( $P$ ) determined, for each replicated chamber ( $n = 3$ ), from the methane decline slope (Slope), the total chamber volume ( $V_{\text{tot}}$ ), the initial concentration gradient between outside and inside ( $C_0 - C_{\text{atm}}$ ) and the gas exchange surface ( $S_c$ ).  $D$  = metallic cylinder diameter,  $L$  = peripheral length of the enclosure,  $H$  = height,  $T$  = thickness,  $C_0$  = initial enclosure concentration,  $C_{\text{atm}} = 1.8951$  ppmv,  $R^2$  = coefficient of determination of the decline regression,  $V_c$  = volume of the chamber,  $V_{\text{tot}} = V_c + V_{\text{dead}}$ ,  $V_{\text{dead}}$  = dead volume of the analyser plus the tubes = 416 cm<sup>3</sup>. Values in brackets represent the standard error of the mean ( $\pm$ SEM).

Enclosure type	$D$ (cm)	$L$ (cm)	$H$ (cm)	$T$ (cm)	$S_c$ (cm <sup>2</sup> )	$V_c$ (cm <sup>3</sup> )	$V_{\text{tot}}$ (cm <sup>3</sup> )	$C_0$ (ppmv)	Slope (mg m <sup>-3</sup> s <sup>-1</sup> ) $\times 10^{-4}$	$R^2$	$P$ (m s <sup>-1</sup> ) $\times 10^{-7}$
Small sleeve	15	25	16	1.5	330	550	966 <sup>a</sup>	109.12 (2.00)	-21.40	0.930	8.30 (0.85) <sup>d</sup>
Large sleeve	15	30	24	1.5	594	990	1406 <sup>b</sup>	71.43 (1.14)	-9.86	0.922	4.77 (0.64) <sup>e</sup>
Rigid chamber	15	28	30	6.5	1413	13165	13581 <sup>c</sup>	9.58 (0.16)	-0.82	0.931	14.62 (1.86) <sup>f</sup>

Volume inaccuracies: <sup>a</sup>  $\pm 3.4\%$ , <sup>b</sup>  $\pm 2.4\%$ , <sup>c</sup>  $\pm 4.1\%$ ; Permeability inaccuracies\*: <sup>d</sup>  $\pm 3.7\%$ , <sup>e</sup>  $\pm 2.8\%$ , <sup>f</sup>  $\pm 4.3\%$ ; \* Calculated from the error propagation formula:

$$\frac{dP}{|P|} \leq \sqrt{\left(\frac{dC}{C}\right)^2 + \left(\frac{dV}{V}\right)^2 + \sqrt{dC^2 + dC_{\text{atm}}^2}} \cong \sqrt{\left(\frac{dV}{V}\right)^2 + 2}$$

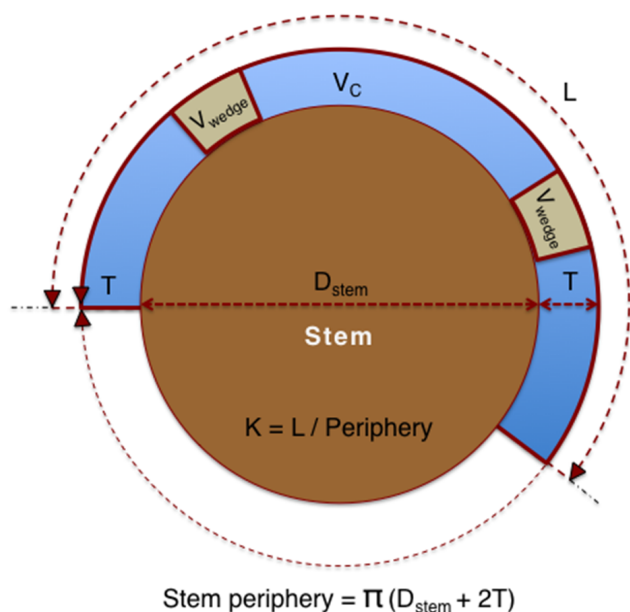


**Figure 4.** 2-D Layout for the chamber volume ( $V_c$ ) calculation based on the stem diameter ( $D_{\text{stem}}$ ), the thickness of the chamber ( $T$ ), the sector covered by the chamber ( $K$ ) and the volume of the wedges ( $V_{\text{wedge}}$ ). Refer to the text for the volume calculations.

ferred it into pre-evacuated glass Exetainers (Labco Ltd, Ceredigion, UK) before analysing CH<sub>4</sub> concentrations on a Fast Methane Analyser (Los Gatos Research Inc., Mountain View, USA) equipped with a sampling loop as described in Baird et al. (2010).

## 2.4 Gas analyses

For the permeability tests, the CH<sub>4</sub> concentration change was analysed in the laboratory under SATP conditions for three types of chamber (Tables 1, S1 in the Supplement); a rigid chamber and two semi-rigid sleeves. We injected 50 mL of a 2000 ppmv methane standard (Air Liquide, Paris) into these chambers after which the CH<sub>4</sub> concentration decline

was measured over 20 min in continuous flow mode. Each chamber type was tested in triplicate. For the blanks, we injected ambient air. The slopes were measured from a linear regression of declining concentrations starting after an equilibration time of 90 s (dead band) and running for 20 min. This dead band represents a maximum time for the continuous flow circuit to mix the entire headspace ( $V_{\text{tot}}$ ).

In the field, the CH<sub>4</sub> concentration changes of a larger sleeve were monitored when deployed on various tree-stem species (see chamber deployment). In order to have a set of contrasting responses we selected, a posteriori, measurement runs with both high and low rates, and also included runs where leakages of the sleeve were present (Figs. 5 and 6, Tables S3 and S4). Methane concentration accumulations were measured as in the laboratory although with shorter runs of approximately 420 s. In the manual sampling mode with syringe, the accumulation period was 900 s. The slopes were measured from linear, quadratic and exponential regressions of increasing concentrations starting after a dead band of 90 s. The gas pressure, temperature and humidity inside the stem sleeve were measured from the circulated gas running through the UGGA's flow-cell and we used temperature, pressure and humidity compensated CH<sub>4</sub> concentrations for the slope calculations. The advantage of using the cell temperature is the perfect synchronicity of the airflow with the temperature measurement. In previous tests we showed that the cell temperature was strongly correlated ( $R^2 = 0.994$ ) to the chamber temperature measured with a small data logger (ST-171, Clas Ohlson, Insjön, Sweden). Besides, the analytical laser did not significantly increase the temperature of the closed circuit (cell, connection tubes and chamber), as the temperature drift over 20 min of enclosure was only +0.7 % under lab conditions (SATP). The chamber pressure was equilibrated to the outside monitored atmospheric pressure (Gas pressure sensor, Vernier, Beaverton, USA) via the vent tube.

All chambers were connected to an UGGA via two flexible tubes (see chamber designs section) set in parallel in a continuous flow mode; one tube bringing air from the gas analyser towards the chambers and the other tube pumping

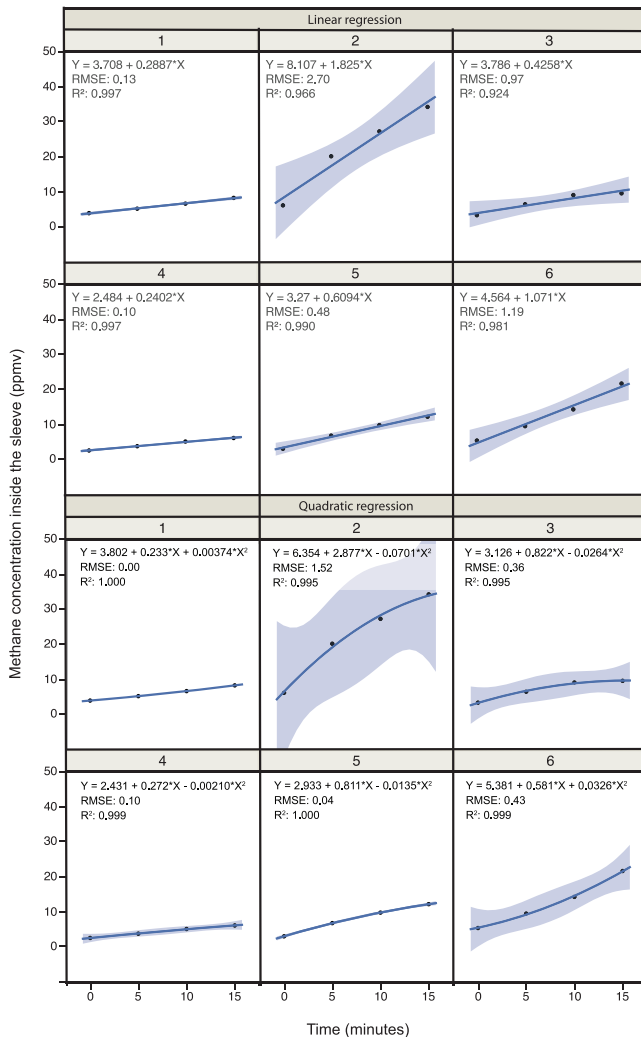


**Figure 5.** Contrasting methane concentration changes in the semi-rigid sleeve from enclosed gas samples measured in a manual mode (syringe) from tree stems. In the first six runs (top quadrants) the concentration changes were regressed with a linear fit, while in the second set of runs they were regressed with a quadratic fit (non-linear). All runs 1–6 were measured on *Heisteria concinna* stems from a tropical lowland forest. The blue line corresponds to 95 % confidence intervals, RMSE = root mean square error,  $R^2$  = coefficient of determination,  $Y$  = methane concentration in ppmv.

air from the headspaces towards the gas analyser. The tubes were connected to the gas analyser via two 1/4 inch push-connect fittings. The UGGA's pump ensured a continuous flow of 2–4 L min<sup>-1</sup>. The UGGA measured CH<sub>4</sub> with the Off-Axis Integrated Cavity Output Spectroscopy (OA-ICOS) at a frequency of 0.33 Hz. The analyser's uncertainty in the range of 0.01 to 100 ppmv of methane is < 1 % without calibration and the precision is ±0.6 ppb over a period of 100 s (LGR, 2013).

## 2.5 Methane permeability calculations

In order to quantify and compare CH<sub>4</sub> losses from the three types of chambers (two semi-rigid sleeves and one rigid chamber) attached to an inert stainless steel cylinder we corrected the loss rates by taking into account both the stem exchange surface covered by each sleeve (or chamber) as well as the concentration gradient between inside and outside of each chamber. To express this we calculated the permeability as a function of the effluxes (outgoing fluxes) and the concentration gradient between inside and outside the chambers.

In the first step we multiplied the slope (mg m<sup>-3</sup> s<sup>-1</sup>) by the total volume of the chamber ( $V_{\text{tot}}$ ) to get the loss rates (mg s<sup>-1</sup>). We then divided the loss rates from each sleeve (or chamber) by the stem exchange surface ( $S_c$ ) covered by each sleeve (or chamber) to express the methane flux ( $J$ ) which can be used for both the permeability experiment on the metallic cylinder and the methane accumulation runs from tree stems in the field:

$$\text{Loss rate} = \text{slope} \times V_{\text{tot}} = \frac{dC}{dt} \times V_{\text{tot}} \left[ \frac{\text{mg}}{\text{s}} \right] \quad (7)$$

$$\text{Flux } (J) = \frac{\text{Loss rate}}{S_c} = \frac{dC}{dt} \times \frac{V_{\text{tot}}}{S_c} \left[ \frac{\text{mg}}{\text{m}^2 \text{ s}} \right]. \quad (8)$$

In the second step, from Fick's first law (Fick, 1855) we could apply the general equation often used in cell biological or textile fabric applications (Ogulata and Mavruz, 2010) to calculate, for each sleeve (or chamber), the CH<sub>4</sub> permeability ( $P$ ) through a porous medium by dividing the CH<sub>4</sub> flux ( $J$ ) by the CH<sub>4</sub> concentration gradient ( $\Delta C$ ) between inside ( $C_{\text{chamber}}$ ) and outside of the sleeve ( $C_{\text{atm}}$ ). We assume that the diffusive CH<sub>4</sub> losses (including dilutions) through the rigid and semi-rigid material are negligible at SATP conditions (McKeen, 2012). Thereafter the equation was

$$J = -P \times \Delta C \rightarrow \text{Permeability } (P) = - \frac{J}{(C_{\text{chamber}} - C_{\text{atm}})} \left[ \frac{\text{m}^3}{\text{m}^2 \text{ s}} \right]. \quad (9)$$

## 2.6 Numerical analyses

We used linear, quadratic and exponential regressions to fit the CH<sub>4</sub> concentrations as a function of the accumulation time in the chambers. The fitting was based on sum of squares' minimisation of the errors. The frequency distribution, homogeneity and homoscedacity of the residuals were previously checked using normal quartile plots, residual versus predicted plots, and box plots. The coefficient of determination ( $R^2$ ) was used to quantify the level of fit. All the data were analysed with the SAS software (SAS Institute Inc., Toronto, Canada).

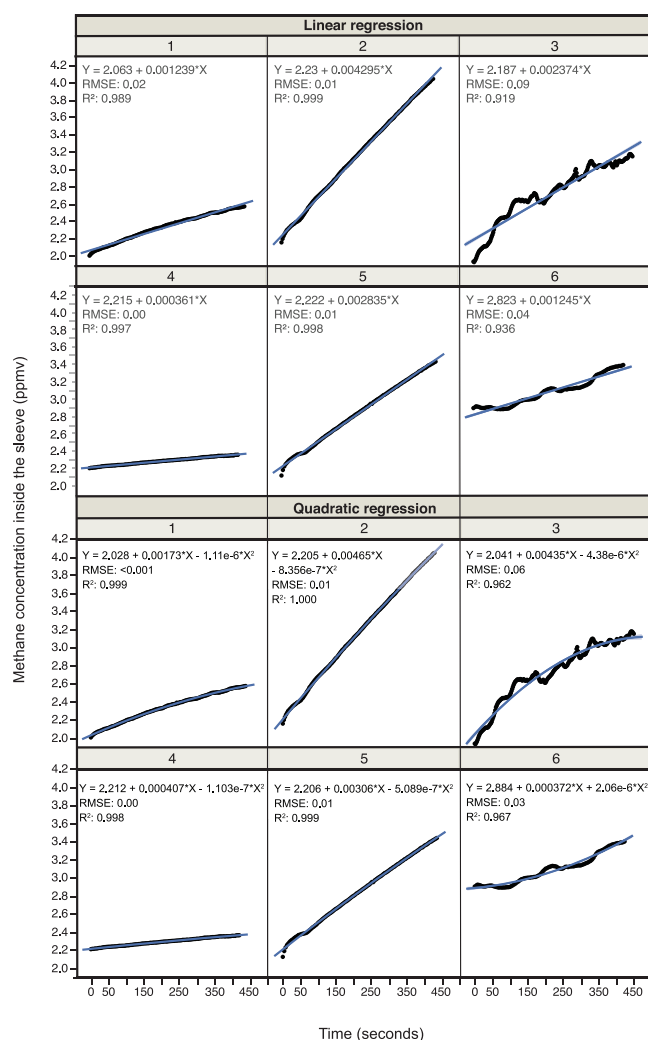


**Figure 6.** Contrasting methane concentration changes in the semi-rigid sleeve from enclosed gas samples measured in continuous flow mode (UGGA) from tree stems. In the first six runs (top quadrants) the concentration changes were regressed with a linear fit, while in the second set of runs (bottom quadrants) they were regressed with quadratic fit (non-linear). Runs 1, 2, 3, and 5 were made on *Betula pendula* stems, runs 4 and 6 were made on *Pinus sylvestris* stems, runs 3 and 6 show the concentration responses in situations where the sleeves were leaking. The blue line corresponds to 95 % confidence intervals, RMSE = root mean square error,  $R^2$  = coefficient of determination,  $Y$  = methane concentration in ppmv.

### 3 Results

#### 3.1 Calibration of the semi-rigid sleeves

The compared predicted (theoretical) and the mean observed empirical  $V'_{\text{tot}}$  (Eqs. 1 and 4) were, respectively, 966 and 933 cm<sup>3</sup> for the small sleeve, 1406 and 1439 cm<sup>3</sup> for the large sleeve, and 13 581 and 13 026 cm<sup>3</sup> for the rigid chamber (Table S1). The observed  $V'_{\text{tot}}$  values included variability due to the possible but very tiny compaction of the Neoprene foam

over the whole frame. This compaction was less than 3 % of  $V_{\text{tot}}$ , which was a maximum considering the pulling force of 200 N applied on the straps (twice 100 N).

The difference between the mean observed  $V'_{\text{tot}}$  and the predicted  $V_{\text{tot}}$  values gave us an estimate of the bias in size. By dividing the absolute value of the bias through the predicted value we get an estimate of the inaccuracy of  $V_{\text{tot}}$  (chamber, tubes and detector's cell). As all terms of the fraction (Eq. 4) are linearly dependent, the inaccuracy of the permeability ( $P$ ) is the quadratic mean of all other terms (Table 1, footnote). The gas exchange surface ( $S_c$ ) could be precisely determined and we assume that there is no error associated with it. The inaccuracies in the concentration measurements are dependent on the uncertainty of the UGGA, which in our case was < 1 % for the un-calibrated device.

The precision of our measurement system, related to repeatability, is the level to which repeated measurements show the same results under the same conditions. For each sleeve or chamber we repeatedly injected 50 mL of a 200 ppmv standard and measured the initial concentration ( $C_0$ , Tables 1, S1) in the enclosed volume. We used the relative standard error (RSE) of the initial concentration ( $C_0$ ) to express the level of precision between different types of chambers. Thereafter, precision is of  $\pm 1.82$  % for the small sleeve,  $\pm 1.59$  % for the large sleeve and  $\pm 1.68$  % for the rigid chamber.

#### 3.2 Chamber permeability comparisons

The comparison of permeability (Tables 1, S1) of the three types of chamber shows that the semi-rigid sleeves are on average less permeable than the rigid chamber, and that the smaller semi-rigid sleeve had a higher permeability compared to the larger one. It was also interesting to note that the CH<sub>4</sub> loss (negative slope) is lower for the rigid chamber compared to semi-rigid sleeves. The contrasting higher permeability of the rigid chamber was counterbalanced by the much greater  $V_{\text{tot}}$  as well as a much lower initial concentration gradient between inside and outside of the chamber ( $dC = C_0 - C_{\text{atm}}$ ). The rigid chamber was 14.1 times that of the small sleeve in volume and 9.7 times that of a large sleeve, and the initial concentration gradient in the rigid chamber was only 1/14 of that in the smaller sleeve and 1/9 of that in the bigger sleeve. Moreover, the larger sleeve had a larger  $S_c$ -to- $V_{\text{tot}}$  ratio (0.42) compared to the smaller sleeve (0.34).

In order to understand why the permeability of the semi-rigid sleeves was lower than that of the rigid chamber we compared and calculated the potential contact distances between air from inside and outside of the chamber volumes (Fig. 3, Table S2). Those contact zones represented the paths where gas effusion could occur, which were driven by the architecture of the chamber. For that purpose we distinguished two types of contact lines: (1) mobile lines that needed to be sealed properly every time the chambers were deployed

and from which most of the losses were likely to occur, and (2) fixed lines that resulted from the manufacture which could be cracked and leak as a result of twisting forces on the rigid joints. The result was that for the same theoretical stem gas exchange surface ( $S_c$ ) between the two chambers (same length and height), the ratio between the length of the mobile lines and the stem gas exchange surface ( $S_c$ ) was 2.17 times smaller for the semi-rigid as compared to the rigid approach.

### 3.3 Stem-methane emissions and field deployments

In the field, the manual sampling by syringe showed steady concentration changes with the sleeve technique (Fig. 5, Table S3), and the linear fitting of those concentration changes was always high ( $R^2 \geq 0.924$ ). When applying a quadratic fit the coefficient of determination improved substantially ( $R^2 \geq 0.995$ ). In continuous flow mode the concentration changes were also consistent with the sleeve technique (Fig. 6, Table S4), and the linear fitting was very high ( $R^2 \geq 0.989$ ) for all the runs not displaying leakages. Equally to the manual sampling mode, in continuous flow mode, the fitting improved slightly when applying a quadratic function or an exponential function ( $R^2 \geq 0.998$ ).

The two modes also distinguish themselves by the fact that with the continuous flow mode the runs are shorter compared to the manual mode. The runs were set to 15 min closure for the manual mode and to 7 min closure for the continuous flow mode. These times included a maximum of 90 s equilibration time just after the sleeve was deployed to allow the headspace to mix properly.

Runs 3 and 6 of the continuous flow mode were deliberately presented to display situations where leakages from sleeves were occurring when placed on *Betula pendula* or *Pinus sylestris* tree stems (Fig. 6). In those cases, the CH<sub>4</sub> concentrations developed in a disordered way with periods of increases immediately followed by sudden drops. These analytically monitored leakages were confirmed when checking the chamber fitting on the stems.

The determination of the coefficient of variation of the root mean square error CV(RMSE), often used to measure the relative differences between two populations of values, and which was calculated between the linear fitted slopes and the non-linear fitted slopes, was higher in the case of the manual sampling mode (0.69) as compared to the continuous flow mode (0.45). In other words, the difference between the linear and non-linear fittings was 53 % higher in the manual mode as compared to the continuous mode. This went in parallel with the differences between the average slope in the linear fitting and that from non-linear fitting which was 27 % higher with the manual sampling mode as compared to 18 % with the continuous mode.

## 4 Discussion

### 4.1 Semi-rigid sleeve construction

The semi-rigid sleeves are easy to assemble, lightweight, and can be locally sourced. The sleeves could easily be assembled on-site following transportation. This allows for minimal luggage or shipping space and low costs, a major asset in terms of logistics where remote fieldwork is concerned. The PET or PC sheets were precisely cut in advance whereas the framing with the Neoprene strips was done on-site. We made sure that all components were not emitting CH<sub>4</sub>, which might otherwise confound in situ measurements. Nevertheless, the raw materials are commonly available internationally, could be found on-site and likewise tested. For small sleeves (stem diameters  $\leq 15$  cm) and middle-sized sleeves (stem diameters  $\leq 25$  cm) the pre-shaped PET sheet can easily be constructed from soft drink PET bottles or PC water-fountain tanks. Larger sleeves (stem diameters  $> 25$  cm) can be built from flat PC sheets as the curvature and volume stability of the chamber becomes less compromised with larger stem diameters. Most important for the construction of the sleeves are the vertical wedges that keep the sheet equidistant from the stem along the radial periphery of the sleeve. The construction of a sleeve took about 1 hour and there was no requirement for specific machine tools and no adhesives were needed, as the Neoprene bands used were adhesive backed. For the production of large numbers of sleeve rectangular plastic sheets could be thermoformed using a specially designed mould (Throne, 1996).

The average CH<sub>4</sub> mass losses (2.2–3.3 %) from the sleeves after 20 min of deployment were 2 orders of magnitude greater as compared to the 0.038 % mass loss after 30 min of deployment reported by Hutchinson and Livingstone (2001) for a perfectly sealed chamber with a sole vent tube. Thereafter, our downscaled vent tube was proportioned to the CH<sub>4</sub> losses from the sleeves.

### 4.2 Calibration of the semi-rigid sleeves

All the chambers were reasonably precise (repeatable) in terms of total volume and the semi-rigid chambers (sleeves) performed equally compared to the rigid chambers. In terms of total volume inaccuracy, all chambers were below the threshold significance level of 5 %. Moreover, the semi-rigid sleeves' total volume accuracy increased with increasing  $S_c / V_{\text{tot}}$ . Nevertheless, getting good accuracy is a matter of calibration as biases can be subtracted from the original readings.

The average 33 cm<sup>3</sup> greater  $V'_{\text{tot}}$  values as compared to  $V_{\text{tot}}$  for the large sleeve (Table S1) can be attributed to the volume of the wedges that were also undergoing a compaction when deployed as the interior periphery gets compressed. This tiny volume correction was not inserted in formula 4 for the sake



of simplicity and because the difference with the calibration was still below 5 %.

We added a known amount of CH<sub>4</sub> instantaneously to the chambers and followed its decline and associated chamber permeability. Thereafter, we can be aware of how well the chambers are doing in keeping the considered gas but not how well they do in minimizing the errors associated with the gas exchange processes between stems and the chamber. For those errors we referred to recommendations from other studies, such as the following: ensuring air-mixing, venting, reducing closure times, reducing chamber volume and considering non-linear fitting (Christiansen et al., 2011; Hutchinson and Livingston, 2001; Juszczak, 2013; Pihlatie et al., 2013).

### 4.3 Chamber permeability comparisons

A reasonable mechanistic explanation to the fact that both semi-rigid sleeves were on average 57 % less permeable compared to the rigid chamber (Table 1) could come from the sleeve's smaller proportion of air contact lines between inside and outside the chambers thereby reducing opportunities for gas diffusion to occur. The difference in that proportion is similar in order of magnitude to the difference in permeability (Table S2). Moreover, it is possible that with an ageing rigid chamber the permeability could increase faster than in the case of an ageing semi-rigid sleeve as the proportion of fixed contact lines could be exposed to more cracks and unforeseen reduced air-tightness (Fig. 3, green lines).

This is also in line with the fact that for the same semi-rigid chamber design with the increasing  $S_c$ -to- $V_{tot}$  ratio, thus by increasing frame size, there is a concurrent decrease in the proportion of contact lines as well as a concurrent decrease in permeability. The rigid chamber had a much lower  $S_c$ -to- $V_{tot}$  ratio when compared to the sleeves and showed the greatest permeability. From our observations we can generalise the common trend found for all chamber types by saying that the larger the total volume of a stem chamber is, for a given gas exchange surface, the greater the expected permeability.

With the same logic and by considering the strong leverage effect of the concentration gradient ( $\Delta C$ ) between inside and outside the chamber, the advantage of the larger rigid chamber is that it keeps the concentration gradient more constant during the chamber deployment and therefore minimizes the non-steady-state gas saturation effect of the closed chamber system. However, this advantage loses its importance when semi-rigid sleeves are connected to precise gas analysers with analytical frequencies of up to 10 Hz as the gradient effect can equally be minimized by reducing the closure times to a few minutes. Additionally, by increasing the  $S_c$ -to- $V_{tot}$  ratio by 6 fold compared to rigid chambers and by mixing the enclosed gas through the continuous flow circulation, we also avoided the problems associated with large volume chambers (Hutchinson and Livingston, 2001, 1993).

Nevertheless, the only non-compressible time factor is the sleeve's equilibration period; a 90 s period for the continu-

ous air circulation to mix the entire headspace. This could be shortened by reducing the tube length, increasing the pump's flow-through or by installing a complementary fan if the sleeves were to be built much larger. In any case, the threshold time by which the sleeve headspace is mixed entirely can be monitored graphically while running every sample. Retrospectively, 90 s of equilibration, together with 3 min closure time, conservatively characterised all replicates made for two different sleeve sizes ( $n = 24$ ).

### 4.4 Deployment in the field

As expected, deployment of the semi-rigid sleeve was very straightforward and could be operated by a single person. The fact that the sleeves had a natural tendency to curve (pre-shaped) allowed them to stay in place when initially placed around the stem. This gave the researcher free hands to attach the straps subsequently. The whole setup takes 2 min to install and swapping the sleeves between different stem heights was also done much more efficiently in comparison to the rigid chamber deployment.

In theory all stem sizes could be fitted, the only limitation comes from the stem texture and this is valid for both semi-rigid sleeves as well as rigid chambers. In some situations, the tree bark had large crevices and it was necessary to prepare the stem prior to attachment of the sleeves or rigid chambers. The preparation was made by filling the crevices with mastic or play dough in the shape of a frame before the chamber or sleeve could be sealed to the stem. In some other situations it was enough to increase the thickness of the sleeves to reduce the percentage of uncertainty in the chamber volume ( $V_c$ ). The impact of both crevices and bumps could be assessed with distance measurements made on photos taken on one side of the deployed sleeves.

Using five sleeve sizes it was possible to cover stem diameters ranging from 5 to 127 cm at breast height (DBH). Moreover, in terms of weight the two sleeves we tested were respectively 156 and 297 g, compared to 3.3 kg for the rigid chamber. As a consequence, the whole collection of sleeves fitted in a single backpack and was light to carry.

Under changeable conditions such as varying sunlight intensities we recommend the temperature inside and outside of the sleeve to be measured, and to shade the sleeve. Otherwise, these varying conditions may alter the gas exchange processes between the stem and the atmosphere.

### 4.5 Sampling modes and regression fits

In both cases, for manual sampling and continuous flow (Figs. 5 and 6), methane accumulation rates were better fitted with non-linear functions (quadratic or exponential). This confirms that the sleeve's closure system was sealing properly against the stems, as the headspace concentration change of a closed non-steady-state chamber (static chamber) will always remain non-linear and this is driven by the laws of dif-

fusion (Hutchinson and Livingston, 2001). For the semi-rigid sleeve, the difference between both the  $R^2$  and the slopes between the linear fitted and the non-linear fitted concentration changes were roughly twice as small compared to those reported in the literature for soil chambers (Christiansen et al., 2011; Hutchinson and Livingston, 2001; Juszczak, 2013; Pihlatie et al., 2013).

Furthermore, the impact of the manual syringe sampling on the pressure fluctuation in the sleeve could be somewhat minimised by the fact that the chamber volume ( $V_c$ ), where the actual air mixing occurred, was increased by the additional dead volume added from the analyser and tubing in continuous flow mode. Thus, the total volume ( $V_{\text{tot}} = V_c + V_{\text{dead}}$ ) was increased as much as 76 % with the smaller sleeve. With rigid soil chambers this aspect is often not mentioned as in those cases the dead volume is negligible compared to the large chamber volume. In our case, for the manual sampling, over a 15 min period, we drew 1.8 % of the total volume from the larger sleeve (4 steps of 0.44 %), which in terms of mass loss remains below the significance level of 5 % and could be accounted for if more accuracy is needed. Although the repeated gas sampling minimises somewhat the pressure build up, recent studies have recommended avoiding manual sampling as much as possible because of associated pressure fluctuations (Christiansen et al., 2011; Juszczak, 2013).

The coefficient of variation of the root mean square error CV (RMSE) gave 53 % higher coefficients for the manual sampling mode compared to the continuous flow mode thus indicating that the discrepancy between the linear fitting and the non-linear fitting is higher for the manual sampling mode. Moreover, as reported by some authors, fluxes calculated using linear fitting together with non-steady state chambers could be underestimated by as much as 40 % (Christiansen et al., 2011; Pihlatie et al., 2013; Kutzbach et al., 2007). In our case, the underestimation was 27 % for manual sampling mode and 18 % for the continuous flow mode. As a consequence we would recommend using non-linear fitting (quadratic or exponential) together with manual sampling of the semi-rigid sleeves. In continuous flow mode, it is better to reduce the closure times as much as possible if planning to use linear fitting for greater simplicity. Both measures will contribute to improving line-fitting and estimating CH<sub>4</sub> accumulation rates.

## 5 Conclusions

Although all chamber types performed well, the semi-rigid design had numerous benefits including reduced gas permeability and an optimal  $S_c$ -to- $V_{\text{tot}}$  ratio. Furthermore, they can be easily constructed and transported in multiple sizes, are extremely light, cheap to build and fast to deploy. As an example, in three of our tropical campaigns it was possible to carry a complete collection of semi-rigid sleeves in a single

backpack. The collection covered the sampling of all ecosystem stem-sizes. Alternatively, we could also build the chambers on-site after prior testing of the compounds for background emissions. The PET and PC sheets of the sleeves are sturdy and lasted the duration of the campaigns, while the closed-cell Neoprene strips could be used for several weeks in the field before they needed to be replaced.

Connecting the sleeves in continuous flow mode to fast and precise laser-spectroscopic gas analysers (CRD or OA-ICOS technologies) enables the combined analysis and air mixing of the sleeve's enclosed volume, as well as reducing the closure periods to no-more than 3 min, making linear fitting from initial rates less problematic. To ensure optimal accuracy of the concentration measurements, it is best to calibrate each individual sleeve's total volume by diluting a standard gas in the entire setup (chamber, connectors, tubes and analyser) prior to starting a measurement programme.

Finally, to make good estimates of the global importance of tree-stem CH<sub>4</sub> emissions, it is essential to make measurements that cover all types of trees (species and morphotypes) present within the often remote ecosystems explored. This necessitates great adaptability in the chamber sizing and transport logistics. The semi-rigid sleeves meet these requirements without compromising the quality of the data collected.

**The Supplement related to this article is available online at doi:10.5194/bg-13-1197-2016-supplement.**

*Acknowledgements.* We would like to thank the landscape biogeochemistry group at SLU Umeå for giving us access to their workshop and laboratory. We would also like to thank Róbert Blaško for logistical help. This work was supported by Natural Environment Research Council (NERC) grant number NE/J010928/1 and AXA Research Fund, both to VG.

Edited by: X. Wang

## References

- Baird, A. J., Stamp, I., Heppell, C. M., and Green, S. M.: CH<sub>4</sub> flux from peatlands: a new measurement method, *Ecohydrology*, 3, 360–367, doi:10.1002/eco.109, 2010.
- Bortoluzzi, E., Epron, D., Siegenthaler, A., Gilbert, D., and Butler, A.: Carbon balance of a European mountain bog at contrasting stages of regeneration, *New Phytol.*, 172, 708–718, doi:10.1111/j.1469-8137.2006.01859.x, 2006.
- Christiansen, J. R., Korhonen, J. F. J., Juszczak, R., Giebels, M., and Pihlatie, M.: Assessing the effects of chamber placement, manual sampling and headspace mixing on CH<sub>4</sub> fluxes in a laboratory experiment, *Plant Soil*, 343, 171–185, doi:10.1007/s11104-010-0701-y, 2011.

- Fick, A.: Ueber Diffusion, *Ann. Phys.-Leibzig*, 170, 59–86, doi:10.1002/andp.18551700105, 1855.
- Gauci, V., Gowing, D. J. G., Hornibrook, E. R. C., Davis, J. M., and Dise, N. B.: Woody stem methane emission in mature wetland alder trees, *Atmos. Environ.*, 44, 2157–2160, doi:10.1016/j.atmosenv.2010.02.034, 2010.
- Hari, P., Nygren, P., and Korpilahti, E.: Internal circulation of carbon within a tree, *Can. J. Forest Res.*, 21, 514–515, doi:10.1139/x91-069, 1991.
- Hutchinson, G. L. and Livingston, G. P.: Use of chamber systems to measure trace gas fluxes, in: *Agricultural Ecosystem Effects on Trace Gases and Global Climate Change*, edited by: Harper, L. A., Mosier, A. R., Duxbury, J. M., Rolston, D. E., Peterson, G. A., Baenziger, P. S., Luxmoore, R. J., and Kral, D. M., American Society of Agronomy/Crop Science Society of America/Soil Science Society of America, Madison, WI, USA, Madison, WI, 63–78, 1993.
- Hutchinson, G. L. and Livingston, G. P.: Vents and seals in non-steady-state chambers used for measuring gas exchange between soil and the atmosphere, *Eur. J. Soil Sci.*, 52, 675–682, 2001.
- IPCC: *Climate Change 2007: The physical science basis*, Contribution of working group I to the fourth assessment report of the intergovernmental panel on climate change, Cambridge University Press, Cambridge, UK and New York, USA, 996 pp., 2007.
- Juszczak, R.: Biases in methane chamber measurements in peatlands, *Int. Agrophys.*, 27, 159–168, doi:10.2478/v10247-012-0081-z, 2013.
- Kutzbach, L., Schneider, J., Sachs, T., Giebels, M., Nykänen, H., Shurpali, N. J., Martikainen, P. J., Alm, J., and Wilming, M.: CO<sub>2</sub> flux determination by closed-chamber methods can be seriously biased by inappropriate application of linear regression, *Biogeosciences*, 4, 1005–1025, doi:10.5194/bg-4-1005-2007, 2007.
- Levy, P. E., Meir, P., Allen, S. J., and Jarvis, P. G.: The effect of aqueous transport of CO<sub>2</sub> in xylem sap on gas exchange in woody plants, *Tree Physiol.*, 19, 53–58, doi:10.1093/treephys/19.1.53, 1999.
- LGR: *Ultra-portable greenhouse gas analyzer user manual*, model 915-0011, Los Gatos Reaserch Inc., Mountain View, USA, 84 pp., 2013.
- McKeen, L. W.: *Film Properties of Plastics and Elastomers*, Elsevier, Amsterdam, The Netherlands, 408 pp., 2012.
- Norman, J. M., Kucharik, C. J., Gower, S. T., Baldocchi, D. D., Crill, P. M., Rayment, M., Savage, K., and Striegl, R. G.: A comparison of six methods for measuring soil-surface carbon dioxide fluxes, *J. Geophys. Res.*, 102, 28771–28777, doi:10.1029/97jd01440, 1997.
- Ogulata, R. T. and Mavruz, S.: Investigation of Porosity and Air Permeability Values of Plain Knitted Fabrics, *Fibres & Textiles in Eastern Europe*, 18, 71–75, 2010.
- Pangala, S. R., Moore, S., Hornibrook, E. R. C., and Gauci, V.: Trees are major conduits for methane egress from tropical forested wetlands, *New Phytol.*, 197, 524–531, doi:10.1111/nph.12031, 2013.
- Pihlatie, M. K., Christiansen, J. R., Aaltonen, H., Korhonen, J. F. J., Nordbo, A., Rasilo, T., Benanti, G., Giebels, M., Helmy, M., Sheehy, J., Jones, S., Juszczak, R., Klefoth, R., Lobo-do-Vale, R., Rosa, A. P., Schreiber, P., Serca, D., Vicca, S., Wolf, B., and Pumpanen, J.: Comparison of static chambers to measure CH<sub>4</sub> emissions from soils, *Agr. Forest Meteorol.*, 171, 124–136, doi:10.1016/j.agrformet.2012.11.008, 2013.
- Pumpanen, J., Kolari, P., Ilvesniemi, H., Minkinen, K., Vesala, T., Niinistö, S., Lohila, A., Larmola, T., Morero, M., Pihlatie, M., Janssens, I., Yuste, J. C., Grünzweig, J. M., Reth, S., Subke, J.-A., Savage, K., Kutsch, W., Østreng, G., Ziegler, W., Anthoni, P., Lindroth, A., and Hari, P.: Comparison of different chamber techniques for measuring soil CO<sub>2</sub> efflux, *Agr. Forest Meteorol.*, 123, 159–176, doi:10.1016/j.agrformet.2003.12.001, 2004.
- Rice, A. L., Butenhoff, C. L., Shearer, M. J., Teama, D., Rosenstiel, T. N., and Khalil, M. A. K.: Emissions of anaerobically produced methane by trees, *Geophys. Res. Lett.*, 37, L03807, doi:10.1029/2009gl014565, 2010.
- Rusch, H. and Rennenberg, H.: Black alder (*Alnus glutinosa* (L.) Gaertn.) trees mediate methane and nitrous oxide emission from the soil to the atmosphere, *Plant Soil*, 201, 1–7, doi:10.1023/a:1004331521059, 1998.
- Ryan, M. G.: Growth and maintenance respiration in stems of *Pinus contorta* and *Picea engelmannii*, *Can. J. Forest Res.*, 20, 48–57, doi:10.1139/x90-008, 1990.
- Subke, J. A., Reichstein, M., and Tenhunen, J. D.: Explaining temporal variation in soil CO<sub>2</sub> efflux in a mature spruce forest in Southern Germany, *Soil Biol. Biochem.*, 35, 1467–1483, doi:10.1016/S0038-0717(03)00241-4, 2003.
- Terazawa, K., Ishizuka, S., Sakata, T., Yamada, K., and Takahashi, M.: Methane emissions from stems of *Fraxinus mandshurica* var. *japonica* trees in a floodplain forest, *Soil Biol. Biochem.*, 39, 2689–2692, doi:10.1016/j.soilbio.2007.05.013, 2007.
- Terazawa, K., Yamada, K., Ohno, Y., Sakata, T., and Ishizuka, S.: Spatial and temporal variability in methane emissions from tree stems of *Fraxinus mandshurica* in a cool-temperate floodplain forest, *Biogeochemistry* 123, 349–362, doi:10.1007/s10533-015-0070-y, 2015.
- Teskey, R. O. and McGuire, M. A.: CO<sub>2</sub> transported in xylem sap affects CO<sub>2</sub> efflux from *Liquidambar styraciflua* and *Plantans occidentalis* stems, and contributes to observed wound respiration phenomena, *Trees*, 19, 357–362, 2005.
- Throne, J. L.: *Technology of Thermoforming*, Carl Hanser Verlag GmbH & Co. KG, Munich, Germany, 898 pp., 1996.